Turbidimetric Studies of *Limulus* Coagulin Gel Formation

Thomas P. Moody,* Maribeth A. Donovan,# and Thomas M. Laue*
*Department of Biochemistry and Molecular Biology, University of New Hampshire, Durham, New Hampshire 03824, and #Biotechnology Division, BioWhittaker, Walkersville, Maryland 21793 USA

ABSTRACT The turbidity during trypsin-induced coagulin gel formation was studied over a range of wavelengths. The range of wavelengths used (686–326 nm) also made it possible to investigate the dependence of turbidity on wavelength (the wavelength exponent). Using the results from that work, and structural information on coagulin and the coagulin gel from other studies, a model gel-forming system was designed that consists of species for which the turbidity can be calculated relatively simply. These species include small particles (small in all dimensions relative to the wavelength of incident light); long rods and long random coils (particles that are large in just one dimension relative to the wavelength of incident light); and reflective regions (aggregated material that is large in more than one dimension relative to the wavelength of incident light). The turbidimetric characteristics of the real coagulin gel-forming system are compared with those of the model system.

INTRODUCTION

The blood of the horseshoe crab *Limulus polyphemus* gels upon contact with Gram-negative bacterial endotoxin (Bang, 1956; Shishikura et al., 1982). Such contact induces the discrete proteolytic cleavage of a single protein, coagulogen. The products are coagulin and a 28-amino acid peptide called the C peptide (Miyata et al., 1983, 1984). The coagulin monomers assemble into a highly turbid gel (Solum, 1970; Takagi et al., 1979; Shishikura et al., 1982). Limited trypsinolysis of coagulogen also produces coagulin (Tai et al., 1977; Liu et al., 1979).

Coagulogen is a single-chain, 175-amino acid, 19,677-Da protein (Miyata et al., 1983, 1984; Cheng et al., 1986). The molecular mass of coagulin calculated from the amino acid sequence is 16,582 Da (Tai et al., 1977; Liu et al., 1979; Cheng et al., 1986). If gelation is initiated by digesting coagulogen with a sufficiently low concentration of trypsin, a lag phase precedes gel formation, suggesting that the self-association of coagulin is a two-step, nucleated polymerization (Timasheff, 1981; Donovan, 1990). It has been hypothesized that helical protofibrils form during the lag phase, during which little increase in turbidity is seen, and that gelation, resulting from a lateral association of the protofibrils, takes place in the following phase, during which a pronounced increase in turbidity is seen (Donovan, 1990). Such a process would be analogous to the formation of soft clots from fibrin (Hantgan and Hermans, 1979; Hantgan et al., 1983). Results are shown here of a turbidimetric study of gelation resulting from the digestion of coagulogen with trypsin. An effort to design a model to reproduce such results is then described.

Received for publication 15 February 1996 and in final form 8 August 1996.

Address reprint requests to Dr. Thomas P. Moody, Department of Biochemistry and Molecular Biology, University of New Hampshire, Durham, NH 03824. Tel.: 603-862-1696; Fax: 603-862-4013; E-mail: tpm@kepler.unh.edu.

0006-3495/96/10/2012/10 $2.00

MATERIALS AND METHODS

Protein preparation

The extraction and purification of coagulogen from *L. polyphemus* was carried out as described by Shishikura et al. (1983), with the removal of *Limulus* trypsin inhibitor as described by Donovan and Laue (1991). Analysis by sodium dodecyl sulfate-polyacrylamide gel electrophoresis (Laemmli, 1970) gave results consistent with a high degree of purity. The protein, in 0.1 M NH_4HCO_3, pH 8, was lyophilyzed and stored at −20°C. No degradation was observed after storage for over a year under these conditions.

Solution preparation

Reagent-grade materials were used. Stock coagulogen solutions were prepared by dissolving the lyophilized protein in 20 mM Tris-HCl (pH 8). Undissolved protein was removed by centrifugation for 140 s at a relative centrifugal force of 16,000 × *g* in a Brinkman Eppendorf centrifuge. The supernatant was passed through a 0.22-μm Millipore Millex-GS filter. Solutions at the desired coagulogen concentration were prepared by dilution of the stock solution with buffer that also had been passed through a 0.22-μm filter.

Turbidimetry

The optical density (OD) of a solution undergoing coagulin gel formation was monitored with a Hitachi U-2000 spectrophotometer. The turbidity, τ, is equal to the OD times the natural logarithm of 10 (Cantor and Schimmel, 1980). Turbidimetry has been used to monitor the mass concentration of polymer in a variety of polymer-forming systems (Johnson and Borisy, 1979; Andreu and Timasheff, 1986; Chou et al., 1990).

The OD of the initial coagulogen solution was measured at 280 nm and 360 nm and at 40-nm intervals from 686 to 326 nm. The filtered buffer used to prepare the solution was used as the reference. Except where noted, the wavelengths of light given are those of light in a vacuum. The OD_λ or τ_λ is the optical density or turbidity, respectively, at a given wavelength, λ. Both initially and during gelation, 0.35 × 0.5 cm masks were used in front of the cuvettes containing the reference and the sample. The light path through the cuvettes was 1 cm. The distance from the cuvettes to the detectors was approximately 6 cm. The photosensitive area on the photodiode of the U2000 is 0.58 × 0.58 cm. The width of the illuminated area at the photodiode is approximately 0.13 cm, and its height, unmasked, is about 0.70 cm.

During gelation, solutions were scanned from 686 to 326 nm, with the OD recorded at 40-nm intervals. By using a scan rate of 1200 nm/min,

scans could be made as frequently as every 30 s. Change in turbidity, $\Delta\tau_\lambda$, was calculated as τ_λ at some time t during the reaction, minus τ_λ at the start of the reaction ($t = 0$). The wavelength exponent was studied by two methods. In one method, it was estimated from the slope of a linear regression fit of $\ln(\tau)$ versus $\ln(\lambda)$ (Gaskin et al., 1974; Johnson and Borisy, 1979; Chou et al., 1990). In this paper the wavelength exponent obtained in this manner is referred to as the global wavelength exponent, or global w. The wavelength exponent as a function of wavelength, $d\ln(\tau)/d\ln(\lambda)$, was also investigated, and is referred to here simply as the wavelength exponent, or w.

A water bath connected to a water-circulated cuvette holder was used to control the temperature of the protein solution in the spectrophotometer. A water-circulated test tube, located outside of the spectrophotometer and containing additional protein solution, was attached to the water bath in series with the spectrophotometer. Before gelation was initiated, the coagulogen solution and all components were equilibrated to temperature.

Gelation was initiated with 9.2 μl of 0.1 mg/ml or 0.01 mg/ml Sigma type XIII *N*-Tosyl-L-phenylalanine chloromethyl ketone-treated bovine pancreatic trypsin in 1 mM HCl per 700 μl of coagulogen solution. This resulted in a final trypsin concentration of 1.3 μg/ml (56 nM) or 0.13 μg/ml (5.6 nM). The time at which trypsin was added to a coagulogen solution was used as time 0 for the gelation. The trypsin solutions were not filtered. Instead, a 1.3 μg/ml trypsin solution was prepared by adding the 0.1 mg/ml trypsin in 1 mM HCl to filtered 20 mM Tris-HCl buffer (pH 8) in the above proportions, and its OD was measured from 700 to 200 nm in the Hitachi U2000 spectrophotometer using the filtered 20 mM Tris-HCl buffer (pH 8) as a reference. The OD of the solution was within 0.001 of 0.000 from 700 to near 300 nm, below which contributions to the OD from absorbance were apparent.

Pelleting

Pelleting accompanied turbidimetry to provide an independent means to monitor the mass concentration of gel during trypsin-induced gel formation (Johnson and Borisy, 1979; Andreu and Timasheff, 1986). Immediately before use, the coagulogen solution was centrifuged for 140 s at 16,000 × *g* in a Brinkman Eppendorf centrifuge. Typically, 1.750 ml of solution was prepared in this way. Using only the upper portion of the centrifuged solution, the amount to be reacted was placed in the water-circulated test tube and allowed to equilibrate. The reaction was then initiated by the addition of trypsin, which was mixed into the solution by inverting the test tube three times. Immediately thereafter, a 500-μl aliquot was removed and placed in the cuvette used to monitor turbidity. Subsequently, 200-μl aliquots were removed from the test tube for pelleting at various times during the reaction.

Immediately after removal, each 200-μl aliquot was placed in a 1.5-ml Eppendorf tube that had been kept on ice. The aliquot was then centrifuged for 140 s at 16,000 × *g* in a Brinkman Eppendorf centrifuge. The purpose of cooling the Eppendorf tubes was to slow down the reaction of trypsin, if not gel formation itself, in the aliquots while the aliquots were spun. The temperature of the centrifuge was not controlled.

After centrifugation, 100 μl of the supernatant was removed from the pelleted aliquot and added to a preweighed 100-μl aliquot of acidified buffer (3 μl 1 N HCl per 100 μl 20 mM Tris-HCl buffer (pH 8)) in a preweighed (± 0.01 mg) Eppendorf tube. The supernatant and acidified buffer were then mixed with a vortex mixer. The pH of the acidified supernatants is estimated to have been between 2 and 3. The purpose of acidifying the supernatants was to quench any further trypsin activity and to minimize the turbidity of the sample. (Coagulin gels lose much of their turbidity at low pH (Solum, 1970).) Typically, 10 aliquots were pelleted during a clotting reaction.

It was assumed that the molar extinction coefficient of coagulin is equal to that of coagulogen, and that lowering the pH from 8.1 to 2 has a negligible effect on this value. This latter assumption would be consistent with the negligible effect that such a pH change has on the OD_{280} of coagulogen.

The masses (± 0.01 mg) of the Eppendorf tubes containing the acidified supernatants were measured. The OD_{280} of each acidified supernatant was then measured and, taking the dilution into account, was used to calculate P, the fraction of protein that pelleted, as follows:

$$P = 1 - (m_{total} \cdot A_{sup})/(m_{sup} \cdot A_o), \quad (1)$$

where m_{total} is the mass of the acidified supernatant, A_{sup} is the OD_{280} of the acidified supernatant from which its OD_{360} was subtracted to standardize the data, m_{sup} is the mass of the acidified supernatant minus the mass of the acidified buffer, and A_o is the corrected OD_{280} of the initial coagulogen solution. To obtain A_o, a calculated OD_{360}, equal to 0.007 × OD_{280}, was subtracted from the measured OD_{280}, and the result was multiplied by 0.987 to correct for the dilution caused by adding trypsin. The light path for all spectroscopic measurements was 1 cm.

The mass concentration of pelletable material, C_P, was calculated from the fraction pelleted as follows:

$$C_P = P \cdot C_i \cdot 16{,}582/19{,}677. \quad (2)$$

C_i is the mass concentration of coagulogen at the start of the reaction. C_i is calculated as A_o/ϵ, where ϵ is 0.587 ml/mg-cm, the extinction coefficient of coagulogen estimated from the tryptophan, tyrosine, and phenylalanine content (Nakamura et al., 1976). It is assumed that the mass of pelletable material is equal to the mass of the gel, and that the gel is constructed almost entirely of coagulin monomers. The ratio of the molecular masses of coagulin and coagulogen, 16,582/19,677, is used to correct C_P for the effect of trypsinolysis on the molecular mass of the monomeric units of the gel. It was assumed that at any given time the mass concentration of the gel, [gel], was equal to C_P.

RESULTS

Turbidity, wavelength exponent, and pelleting

Some general features of trypsin-induced coagulin gel formation are illustrated with data from an experiment conducted at 15°C. In Fig. 1, turbidity data from representative times during the reaction are plotted versus wavelength. Figs. 2 and 3 are plots of the change in turbidity at 326 nm ($\Delta\tau_{326}$) and the global wavelength exponent versus time.

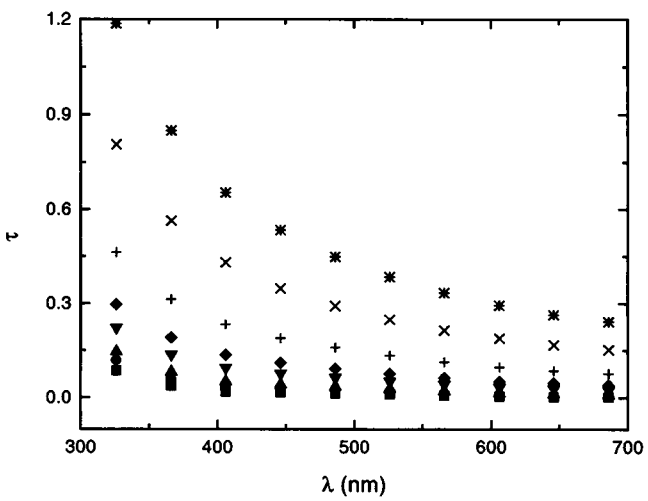

FIGURE 1 Turbidity versus wavelength at selected times during gel formation. Minutes after the addition of trypsin (9.2 μl of 0.10 mg/ml trypsin per 700 μl of solution) to 4.505 mg/ml coagulogen in 20 mM Tris-HCl buffer (pH 8) at 15°C: ■, 1.5; ●, 5.5; ▲, 7; ▼, 8; ◆, 10; +, 14; ×, 22; *, 32.

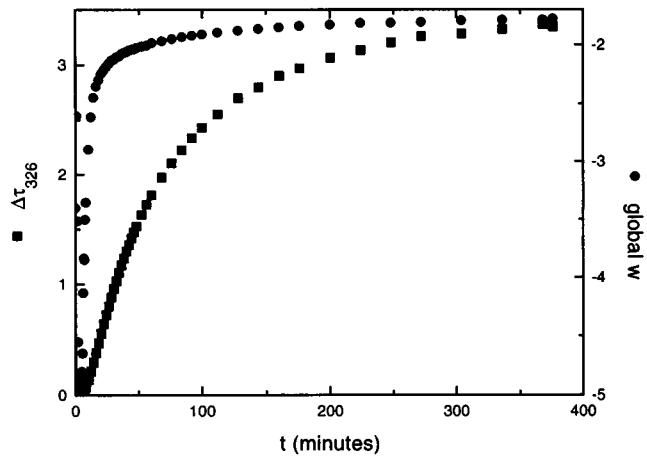

FIGURE 2 Change in turbidity at 326 nm ($\Delta\tau_{326}$) and global wavelength exponent (global w) versus time for the entire reaction. Used 9.2 μl 0.10 mg/ml trypsin per 700 μl of 4.505 mg/ml coagulogen in 20 mM Tris-HCl buffer (pH 8) at 15°C.

Phenomenological reaction kinetics

The data show that turbidity changes more slowly than the global wavelength exponent, although neither changes appreciably during the first 3 min (Fig. 3). In the following 15 min, the global wavelength exponent nears its final value while the change in turbidity is approaching about a fifth of its final value (Fig. 3). During the rest of the reaction, the change in turbidity gradually increases, while the global wavelength exponent is nearly constant (Fig. 2). That these three periods are distinguishable suggests that the gel formation has three discrete phases. The phases can be characterized by $d(\Delta\tau_{326})/dt$, the rate of change in the turbidity. The approach resembles that of De Cristofaro and Di Cera (1991), who applied the maximum in $d(\Delta OD_{350})/dt$ (ΔOD_{350} being the change in the OD_{350} from its initial value) to a phenomenological analysis of thrombin-induced fibrin gel formation. In the initial phase, $d(\Delta\tau_{326})/dt$ is at or near zero. During the second phase, $d(\Delta\tau_{326})/dt$ is positive. The end of the second phase is marked by $d(\Delta\tau_{326})/dt$ reaching its maximum value. In the third phase, $d(\Delta\tau_{326})/dt$ is negative.

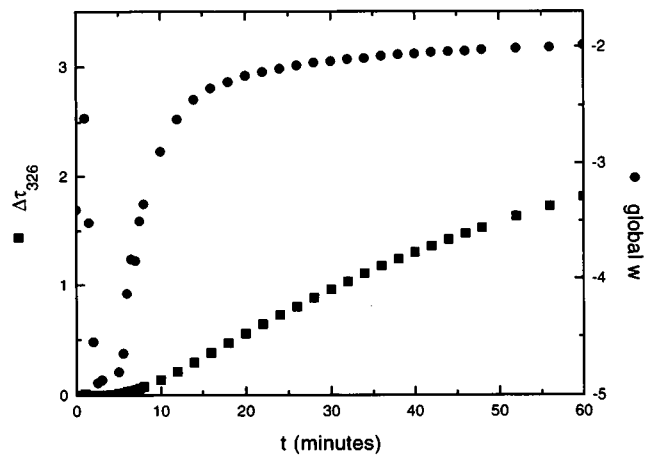

FIGURE 3 Change in turbidity at 326 nm ($\Delta\tau_{326}$) and global wavelength exponent (global w) versus time for the first hour of the reaction. Used 9.2 μl 0.10 mg/ml trypsin per 700 μl of 4.505 mg/ml coagulogen in 20 mM Tris-HCl buffer (pH 8) at 15°C.

Other features also mark the three phases. During the first phase, there is no appreciable change in the global wavelength exponent (Fig. 3). At the beginning of the second phase, however, it changes rapidly (Fig. 3). Shortly after the beginning of that phase, it reaches its maximum value. By the end of the second phase, the time derivative of the global wavelength exponent has dropped almost to zero, where it stays throughout the third phase. The third phase is further marked by a proportionality of the mass concentration of pelletable material, C_P, to $\Delta\tau_{326}$. This is shown by Fig. 4, in which [gel] (assumed to equal C_P) versus $\Delta\tau_{326}$ data from several gel forming-reactions are plotted and fit by linear regression. The experiments were all conducted at 15°C, although the initial concentration of coagulogen varied. Data from these same experiments suggest that the proportionality of C_P to $\Delta\tau_{326}$ in the second phase may not be the same as it is in the third phase (data not shown). The most that can be said is that pelletable material appears to be present during the second phase. Because of the brevity of the first phase, few pelleting data could be obtained during that period.

When the amount of trypsin used to initiate the reaction was reduced from 56 nM to 5.6 nM, the first phase, which, judging by its characteristics, is the lag phase, lengthened and became noticeably dependent on the concentration of

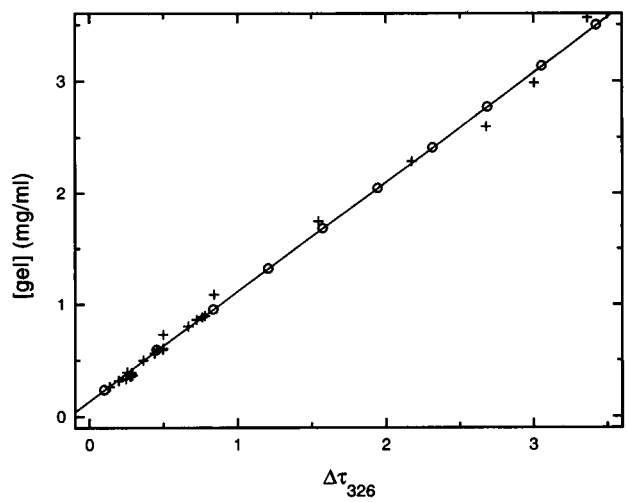

FIGURE 4 Gel concentration versus change in turbidity at 326 nm. +, Data obtained from gel formation reactions conducted in 20 mM Tris-HCl buffer (pH 8) at 15°C using 9.2 μl 0.10 mg/ml trypsin per 700 μl of solution. The initial coagulogen concentration varied. The equation of the line obtained from a linear regression fit of the data is C_P = [gel] = (0.980 ± 0.015 mg/ml) × (1 cm) × $\Delta\tau_{326}$ + (0.137 ± 0.020 mg/ml). ○ Data from the hypothetical reaction (Table 1). The equation of the line obtained from a linear regression fit of the data is [gel] = (0.980 ± 0.001 mg/ml) × (1 cm) × $\Delta\tau_{326}$ + (0.138 ± 0.001 mg/ml).

coagulogen (data not shown). The longer lag phase at lower trypsin concentrations is further evidence that there is a critical concentration or a nucleation event. The critical concentration, however, was found to be too low to measure (data not shown) (Moody, 1994). The dependence of the duration of the lag phase on coagulogen concentration suggests that the K_M of trypsin for coagulogen may be in the range of the coagulogen concentrations used (Rawn, 1983).

DISCUSSION

Choice of species used to model gel formation

Coagulin gel formation begins with the conversion of coagulogen monomers into coagulin monomers (Tai et al., 1977; Liu et al., 1979). From the dimensions of these monomers (Holme and Solum, 1973; Donovan, 1990; Moody, 1994), it is clear that they both should exhibit the light-scattering characteristics of small particles (particles with dimensions that are small with respect to the wavelengths of light used in this study) (Geiduschek and Holtzer, 1958). (Any trypsin molecules present in solution also should behave as small particles, but because of their low concentration in the experiments described here, their scattering effects are ignored.) For small particles, the relationship of turbidity to concentration and molar mass (see Appendix) is well understood (Tanford, 1961; Cantor and Schimmel, 1980; Castellan, 1983).

In contrast with either coagulogen or coagulin monomers, the coagulin gel consists of long, winding, interconnected fibers (Holme and Solum, 1973; Moody, 1994). Although the fibers are thin with respect to wavelengths of light in the visible to near-UV range, they are quite long (Holme and Solum, 1973). For materials with dimensions comparable to, or greater than, the wavelength of light, the wavelength exponent and the relationship of turbidity to concentration and molar mass can be difficult to predict (Timasheff, 1981). Long rods and long random coils (see Appendix) are, however, exceptions in that respect (Zimm, 1948a,b; Doty and Steiner, 1950; Debye, 1954; Geiduschek and Holtzer, 1958; Gaskin et al., 1974).

There also may be regions of the gel that are so large in more than one dimension (relative to the wavelength of incident light), and throughout which the fibers are so densely packed, that light traveling through the solvent is partially reflected when it encounters them (see Appendix).

Small particles, long rods, and long random coils are used here to model some of the turbidimetric characteristics of a solution in which a coagulin gel is forming. Coagulogen, coagulin, and small oligomers of coagulin are assumed to exhibit the turbidimetric characteristics of small particles. Most of the gel is assumed to exhibit the turbidimetric characteristics of a collection of rods and random coils of essentially infinite length relative to the wavelengths of light considered here. In addition, the model of the gel includes another species consisting of a small but significant amount of material that contributes to the turbidity through reflection. The latter species is not linked to reported structures and is invoked to make up for the extent to which the small particles, long rods, and long random coils fall short of explaining turbidimetric observations.

As a first approximation, the turbidity of the model solution is considered to equal the linear sum of the turbidity calculated for each of the various species present (see Appendix). The effects of interparticle interference are neglected. As Fig. 4 shows, however, the turbidity is proportional to the mass concentration of the gel (as measured by pelleting) over a wide range of gel concentrations (approximately 0.2–3.5 mg/ml). This suggests that the second and higher virial terms that would result from interparticle interference (Zimm, 1948a) can be ignored for the coagulin gel concentrations examined in this study. It also suggests that there is no significant amount of multiple scattering (van de Hulst, 1957). The effects of branching structures and the restricted mobility of structures in the gel are also neglected, in so far as the calculation of the turbidity due to long rods and long random coils is concerned. For the sake of simplicity, the long rods and long random coils of the model are treated in the same way they would be if they were free in solution (see Appendix), and it is assumed that the gel formation introduces no ordering of the gel segments that the long rods and long random coils of the model represent. The model, therefore, is admittedly crude.

The turbidimetric properties of the model solution are calculated by applying the appropriate equations for turbidity (see Appendix) to all species of the model. The structural basis for these model species is shown in Fig. 5. The structures in Fig. 5 are consistent with previous work, including studies of the gel by electron microscopy (Holme and Solum, 1973; Moody, 1994) and analytical ultracentrifugation (Donovan, 1990; Moody, 1994). The analytical ultracentrifugation work included studies in which the gel was partially depolymerized by subjecting it to acidic conditions (Donovan, 1990), and studies in which the gel was totally depolymerized in 6 M guanidine HCl (Moody, 1994). The latter work, together with fluorescence studies (Moody, 1994), gave evidence that the coagulin monomer is roughly spherical; hence the monomer is treated as a sphere in Fig. 5.

Some insight into how the coagulin monomers interact to form the gel and precursors of the gel is provided by the manner in which the gel is affected by low pH (Solum, 1970; Donovan, 1990), high pH (Solum, 1970), ionic strength (Moody, 1994), guanidine HCl (Moody, 1994), urea (Solum, 1970), sodium dodecyl sulfate (Solum, 1973; Gaffin, 1976), and reducing agents such as β-mercaptoethanol (Gaffin, 1976). Analytical ultracentrifugation studies (Donovan, 1990; Moody, 1994) have shown that coagulogen weakly self-associates, which is evidence that the peptide removed when coagulogen is converted to coagulin blocks some, but not all, of the interactions of which coagulin is capable. Such information regarding interactions between coagulin monomers was incorporated into the structural model in Fig. 5, details of which will be presented

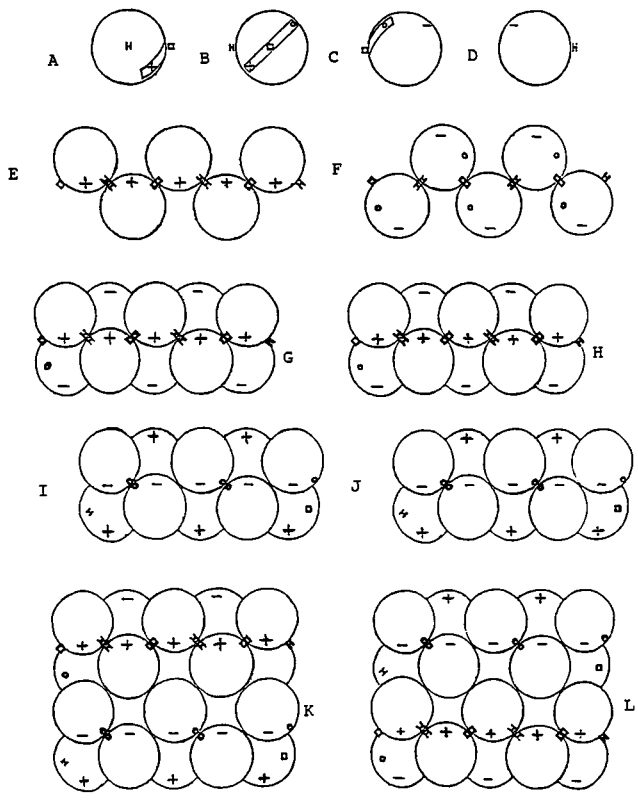

FIGURE 5 Model protofibril. (*A–D*) Four views of the model coagulin monomer. The monomer is a 1.7-nm-radius sphere. Rotating *A* 90° clockwise about its vertical axis gives rise to *B*. Doing the same to *B* yields *C*, and rotating *C* produces *D*. In the model, the C-peptide of coagulogen covers the regions that are shown inside the band seen in *A* through *C*. *E* and *F* are two views of a section of the 3.4-nm-wide strand formed from the model coagulin monomers. Rotating one about the horizontal axis by 180° gives rise to the other. Additional monomers would increase the length of the strand along the horizontal axis. The regions marked by the square and the letter H are those that interact to form the strand. H designates a complementary region that interacts through H-bonds. The square designates another region of the same type. (*G–J*) Four views of the model protofibril that would result from the dimerization of two strands (superposing *E* on *F* produces *G*). The helix width and the periodicity of the protofibril are 5.8 nm. Rotating *G* 180° about the horizontal axis gives rise to *H*. Rotating *I* in this way gives rise to *J*. Rotating *G* 90°, removing two monomers from the left end, and adding two to the right end produces *I*. The same operation on *H* gives *J*. Complementary hydrophobic regions, marked by the circle, are those that interact to form the protofibril. *K* and *L* are sections of laterally associated model protofibrils. *K* is obtained by placing the bottom of *G* on the top of *I* (or by placing *H* on *J*). *L* would result from placing *I* on *G* (or *J* on *H*). The amount by which one protofibril overlaps another with which it is laterally associated is $(2 - \sqrt{2})$ times the radius of the monomer. The dash is a negatively charged region, and the cross is a positively charged region. These are complementary regions that, through ionic interactions, give rise to laterally associated protofibrils.

in a forthcoming paper. Nothing in either that paper or this, however, is meant to suggest that the types of interactions between monomers, the locations of sites of interactions between monomers, the geometry of the monomers with respect to one another in the gel or its precursors, or the geometry of the monomers themselves can be shown to conform to the pattern described in Fig. 5. The structures in Fig. 5 were constructed using existing information for the sole purpose of providing a basis for the calculation of the turbidity of a solution composed of model species that resemble the actual material found in a real solution.

A model of the reaction

The general model used here for coagulin gel formation is as follows:

1. The first phase of the reaction is the lag phase, which involves the formation of nuclei that contribute little to the turbidity of the solution.

2. The second phase is the gel initiation phase, during which the gel network is assembled from newly formed protofibrils. Free protofibrils, and much of the gel network, can be described as a collection of long rods, but the formation of the gel network also gives rise to long random coils. As this phase progresses, reflective regions also appear. The ratio of the mass of the long rods to the total polymer mass decreases with time, and the mass ratios of the long random coils and reflective regions increase with time. The changing mass ratios of these species cause the wavelength exponent for the turbidity of the solution (Eq. A.26) to change over the course of this phase from -4.754 to -2.774 at a wavelength of 326 nm, and from -4.193 to -1.333 at 686 nm (these values are taken from Table 1). During this phase and the next, polymerization can occur not only through the addition of monomers to the ends of protofibrils, but through the lateral association of protofibrils as well (Fig. 5).

3. The third phase is the gel propagation phase, which begins just as the wavelength exponent has nearly ceased changing. The wavelength exponent is nearly constant in this phase because the mass concentration of each highly turbid species (the long rods, long random coils, and reflective regions) is a constant fraction of the mass concentration of the gel. The gel propagation phase involves the direct association of coagulin monomers with the gel network, together with the continued formation of protofibrils, which quickly become incorporated into the gel. Using this model and the appropriate equations for turbidity and the wavelength exponent (see Appendix), turbidimetric properties are calculated that are similar to those observed in actual experiments.

In Table 1, turbidimetric characteristics are shown for a hypothetical reaction that fits the pattern of the model described above. The total protein concentration is set at 3.535 mg/ml. Coagulin monomer and coagulogen monomer are considered identical as far as their scattering properties are concerned. Oligomers, which are grouped with the small particles, are all considered to be 22 mer of coagulin. The oligomer concentration never exceeds 0.001 mg/ml at any point during the reaction. Throughout the gel propagation phase, 95.8% of the mass concentration of the gel consists of long rods, 3.19% consists of long random coils, and 0.991% consists of the reflective species. The weight-aver-

TABLE 1 Hypothetical reaction data

C_{small}	C_{rr}	C_{rod}	C_{coil}	$\langle X \rangle$	τ_{326}	$-w_{326}$	τ_{686}	$-w_{686}$
3.535	0	0	0		0.002	4.754	0.0001	4.193
3.434	*0*	*0.100*	*0.001*	*1.200*	*0.017*	*3.482*	*0.002*	*2.756*
3.297	0.002	0.228	0.008	1.455	0.103	2.774	0.023	1.333
2.938	0.006	0.572	0.019	2.622	0.458	2.741	0.102	1.325
2.571	0.010	0.924	0.031	2.975	0.837	2.736	0.186	1.324
2.203	0.013	1.276	0.042	3.112	1.208	2.735	0.269	1.324
1.836	0.017	1.628	0.054	3.187	1.578	2.734	0.351	1.323
1.470	0.020	1.979	0.066	3.235	1.946	2.733	0.434	1.323
1.102	0.024	2.331	0.078	3.270	2.317	2.733	0.516	1.323
0.735	0.028	2.683	0.089	3.297	2.688	2.733	0.599	1.323
0.368	0.031	3.035	0.101	3.317	3.059	2.732	0.682	1.323
0.002	0.035	3.386	0.113	3.334	3.429	2.732	0.765	1.323

C_{small} is the mass concentration of small particles (coagulogen, coagulin monomers, and small oligomers), C_{rod} is that of long rods, C_{coil} that of long random coils, and C_{rr} that of the reflective species. All concentrations are in mg/ml. The concentration of small oligomers (22 mer) is 0.001 mg/ml throughout. $C_{coil} = 0.0333 \cdot C_{rod}$ and $C_{rr} = 0.01 \cdot (C_{rod} + C_{coil})$, except for the line in italics, where $C_{coil} = 0.01 \cdot C_{rod}$ and $C_{rr} = 0$. The concentration of gel is assumed to equal $C_{rod} + C_{coil} + C_{rr}$. The weight-average degree of lateral association $\langle X \rangle$ is simulated using a modified Gompertz growth curve that is a function of $(C_{rod} + C_{coil})$. The constant C_i is the minimum value that C_{rod} takes on for the concentration range covered by this function (in this instance, $C_i = 0.228$ mg/ml). The maximum value of $\langle X \rangle$ is set at 7.138. The equation for $\langle X \rangle$ is $\langle X \rangle = (7.138/A) \cdot \exp[-0.6 \cdot \exp(-[C_{rod} + C_{coil}]/[B \cdot 200 \cdot C_i])] \cdot (1 - [C_{rod} - C_i]/[D \cdot C_{rod}])$, where $A = 2.7^{\wedge}(C_i/C_{rod})$, $B = 2000^{\wedge}(1 - C_i/C_{rod})$, and $D = 8.18 + 100{,}000^{\wedge}(C_i/C_{rod})$. The turbidity at 326 nm is τ_{326}, and that at 686 nm is τ_{686}. The wavelength exponent at 326 nm is w_{326}, and that at 686 nm is w_{686}. The first row of the table is representative of the lag phase. The italicized row represents an instant during the gel initiation phase. The third through twelfth rows represent successive time points during the gel propagation phase; the last row is the end of the reaction, when no coagulogen is left.

age degree of lateral association of the long random coils is equal to that of the long rods at all times (see Appendix) and increases as a function of the sum of the mass concentrations of the two species (Table 1). The weight-averaged degree of lateral association of the reflective species (see Appendix) is also equal to that of the long rods at all times.

In an actual nucleation polymerization reaction there is some critical concentration below which polymerization does not occur (Oosawa and Asakura, 1975). Small oligomers, which are nuclei of the polymers, can form at a concentration below that of the critical concentration, however (Oosawa and Asakura, 1975).

In keeping with results from the actual reaction, the critical concentration for the hypothetical reaction is given a low value of 0.002 mg/ml total mass concentration of coagulin (the mass concentration of coagulin and all polymers of coagulin). Below this concentration, the largest species formed in the hypothetical reaction is a 22 mer, which can be considered the nucleus of protofibril formation. Such a nucleus could be a section of the strands from which the protofibrils are formed (Fig. 5). The formation of a small amount of 22 mer (0.001 mg/ml) during the lag phase of the hypothetical reaction has no significant effect on the turbidity. Thus the hypothetical lag phase exhibits the same characteristics of the actual lag phase. (Kinetic factors beyond the rate of reaction of coagulogen with trypsin may affect the length of the actual lag phase. In the actual reaction, the lag phase probably continues even after the critical concentration has been substantially exceeded. If not, the lag phase would probably be too short to observe at the higher of the two trypsin concentrations used in the experiments described here.)

The experimentally observed presence of pelletable material in the second phase is consistent with the presence of a gel network. In the model, therefore, it is during this period, denoted here as the gel initiation phase, that the gel first forms. The gel initiation phase starts when the total mass concentration of coagulin exceeds the critical concentration. Above the critical concentration, the mass concentration of 22 mer and the mass concentration of coagulin monomers each remain unchanged at 0.001 mg/ml. The rest of the coagulin is in the gel. (It should be noted that the total mass concentration of small particles includes the mass concentration of any coagulogen that has not yet reacted with trypsin.)

Equation 3, which relates $\Delta\tau_{326}$ to C_P during the gel propagation phase, was obtained from the linear regression fit of experimental data (Fig. 4):

$$C_P = [0.980 \text{ mg/ml}] \cdot l \cdot \Delta\tau_{326} + 0.137 \text{ mg/ml}. \quad (3)$$

In this equation, l is the pathlength. For the model, turbidity is approximately proportional to [gel] times the weight-average degree of lateral association, $\langle X \rangle$ (see Appendix). Unless this product increases linearly with [gel], the proportionality of turbidity to [gel] at low gel concentrations would be different from that at high gel concentrations (Timasheff, 1981; Andreu and Timasheff, 1986). Thus, a function for $\langle X \rangle$ was devised such that [gel] times $\langle X \rangle$ is approximately linear with [gel] during the gel propagation phase (Table 1). The degree of lateral association of the model coagulin gel is designed to resemble that of the fibrin gel, in which a maximum weight-average degree of lateral association is approached as the mass concentration of gel increases (Weisel et al., 1987).

The relationship between $\Delta\tau_{326}$ and [gel] for the hypothetical system is shown in Fig. 4, which uses the data shown in Table 1. Equation 4, which relates $\Delta\tau_{326}$ to [gel]

during the gel propagation phase of a hypothetical system, was obtained from the linear regression fit of those data:

$$[\text{gel}] = [0.980\ \text{mg/ml}] \cdot l \cdot \Delta\tau_{326} + 0.138\ \text{mg/ml}. \quad (4)$$

Equation 4 is a close approximation of Eq. 3. Hypothetical data for which [gel] is less than 0.239 mg/ml would not pertain to the gel propagation phase and would not behave according to Eq. 4. Such data would belong instead to the gel initiation phase, for which, in a plot of [gel] versus $\Delta\tau_{326}$, [gel] would take on a value of 0 mg/ml at $l \times \Delta\tau_{326} = 0$.

The data in Figs. 6–8 pertain to a point in time during a gel propagation phase. Real data are compared with model data in Fig. 6, which is a plot of τ versus λ; Fig. 7, which is a plot of ln τ versus ln λ; and Fig. 8, in which dln τ/dln λ is plotted against λ. Figs. 6 and 7 suggest that the model data approximate actual data fairly well. Fig. 8 shows the extent to which the wavelength exponent of model data matches that of actual data.

As a result of their different power laws with respect to wavelength (see Appendix), the small particles, long rods, long random coils, and reflective regions, when together in solution, are expected to cause the wavelength exponent to increase as wavelength increases. Dispersion in the refractive index of the solvent and the refractive index increment of the solution also contributes to the increase in the wavelength exponent with wavelength (Doty and Steiner, 1950; Camerini-Otero et al., 1974; Cancellieri et al., 1974; Camerini-Otero and Day, 1978) and accounts for a large part of this effect for the hypothetical data. Without dispersion, the wavelength exponent for the hypothetical data in Fig. 8 would change from −2.029 at λ = 326 nm to −1.180 at λ = 686 nm.

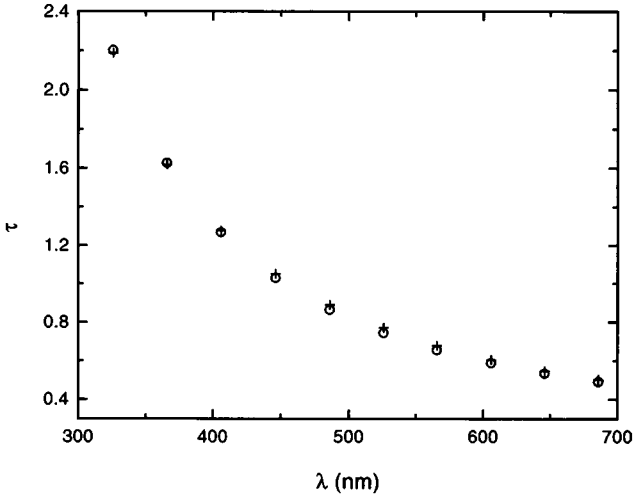

FIGURE 6 Turbidity versus wavelength. O, Hypothetical reaction: ⟨X⟩ = 3.260, [small particles] = 2.187 mg/ml, [long rods] = 2.220 mg/ml, [long random coils] = 0.074 mg/ml, [reflective regions] = 0.023 mg/ml, [total protein] = 4.505 mg/ml: τ_{326} = 2.201. +, Actual reaction, 76 min after adding trypsin (9.2 μl of 0.10 mg/ml trypsin per 700 μl of solution) to 4.505 mg/ml coagulogen in 20 mM Tris-HCl buffer (pH 8) at 15°C: τ_{326} = 2.187.

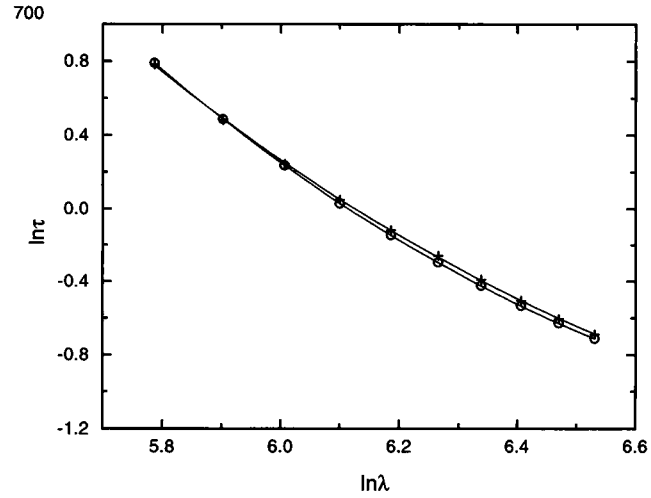

FIGURE 7 The natural log of the turbidity versus the natural log of the wavelength. O, Hypothetical reaction: ⟨X⟩ = 3.260, [small particles] = 2.187 mg/ml, [long rods] = 2.220 mg/ml, [long random coils] = 0.074 mg/ml, [reflective regions] = 0.023 mg/ml, [total protein] = 4.505 mg/ml: global wavelength exponent = −2.001. +, Actual reaction, 76 min after adding trypsin (9.2 μl of 0.10 mg/ml trypsin per 700 μl of solution) to 4.505 mg/ml coagulogen in 20 mM Tris-HCl buffer (pH 8), at 15°C: global wavelength exponent = −1.952.

It is by virtue of the reflective species that the wavelength exponent for the hypothetical data can take on values between −2 and −1. If the mass concentration of reflective regions of the hypothetical data of Fig. 8 were replaced by an equal concentration of small particles, the wavelength exponent would change from −3.068 at λ = 326 nm to −2.522 at λ = 686 nm. This illustrates the importance of the reflective regions, or something like them, to the model

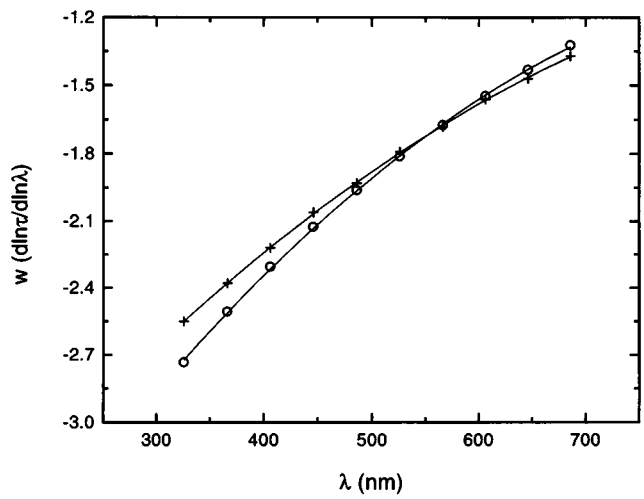

FIGURE 8 Wavelength exponent versus wavelength. O, Hypothetical reaction: ⟨X⟩ = 3.260, [small particles] = 2.187 mg/ml, [long rods] = 2.220 mg/ml, [long random coils] = 0.074 mg/ml, [reflective regions] = 0.023 mg/ml, [total protein] = 4.505 mg/ml. +, Actual reaction, 76 min after adding trypsin (9.2 μl of 0.10 mg/ml trypsin per 700 μl of solution) to 4.505 mg/ml coagulogen in 20 mM Tris-HCl buffer (pH 8) at 15°C.

presented here. Such a species is crucial to matching the turbidimetric properties of the model system to those of the real system.

Even with the reflective regions, the turbidimetric properties of the model system do not match exactly those of the real system. The discrepancy may be due, in part, to the model system lacking some features of the real system, such as a branching, networked gel structure with restricted mobility. The difference may also stem from the effects of low-angle scattering on the experimental results. It is likely that some light scattered at low angle reached the detector of the spectrophotometer, resulting in a reduction of the apparent turbidity. The effect would increase as forward scattering increases, and thus would increase with decreasing wavelength. If this effect were eliminated from the real data, or incorporated into the model, the two systems might give more closely matched results.

APPENDIX

The turbidity of a solution can be described by $\ln(I_o/I)$, where I_o is the intensity of the incident light and I is the intensity of the light transmitted through the solution (Doty and Steiner, 1950). For unpolarized light, the turbidity, τ, per unit of pathlength of a solution of particles of any given shape is

$$\tau = [(32\pi^3 n_o^2(\partial n/\partial C)_\mu^2/(3N_A\lambda^4)] \cdot Q/(1 + 2BMC), \quad (A.1)$$

where n_o is the refractive index of the solvent, n is the refractive index of the solution, N_A is Avogadro's number, λ is the wavelength of the light in a vacuum, M is the molar mass of the particle, C is its mass concentration, Q is its particle dissipation factor, and B is its deviation from van't Hoff behavior (Doty and Steiner, 1950). The refractive increment of the solution at dialysis equilibrium with the solvent is $(\partial n/\partial C)_\mu$ (Casassa and Eisenberg, 1964). The refractive index of the solvent is estimated here as $n_o = a_1(a_2 + a_3/\lambda^2)$, where $a_1 = 1.3346$, $a_2 = 0.9922$, and $a_3 = 2.31 \times 10^{-11}$ cm^2 (Camerini-Otero and Day, 1978). The refractive increment is estimated here as $(\partial n/\partial C)_\mu = b_1(b_2 + b_3/\lambda^2)$, where $b_1 = 0.188575$ cm^3/g, $b_2 = 0.933$, and $b_3 = 1.99 \times 10^{-10}$ cm^2 (Camerini-Otero and Day, 1978). The particle dissipation factor is

$$Q = (3/8)\int P(\theta)(1 + \cos^2\theta)\sin\theta\, d\theta, \quad (A.2)$$

integrated from 0 to π radians, where θ is the scattering angle relative to the forward direction of the incident beam of light and $P(\theta)$ is the particle scattering factor (Doty and Steiner, 1950). The particle scattering factor is equal to 1 for particles that are small in comparison to the wavelength of the incident light (van Holde, 1985). Thus, for B equal to zero, the turbidity of small particles is

$$\tau_{small} = [32\pi^3 n_o^2(\partial n/\partial C)_\mu^2/(3N_A\lambda^4)]MC. \quad (A.3)$$

For long rods of length L, where L is much greater than λ/n_o, x equals $4\pi n_o L \sin(\theta/2)/\lambda$ and the limits of integration are from 0 to $2x$,

$$P(\theta) = (1/x)\int [\sin(s)/s]ds - [\sin(x)/x]^2 \quad (A.4)$$

(Doty and Steiner, 1950; Geiduschek and Holtzer, 1958). According to Berne, for a monodisperse solution of randomly oriented, rodlike molecules, the turbidity should be proportional to the mass concentration of those molecules, provided that they meet two criteria: 1) the thickness of the molecules is small relative to both the wavelength of light and the length of the molecules; 2) the segments of the molecules are optically isotropic and of identical polarizability (Gaskin et al., 1974; Timasheff, 1981). For B equal to zero, the turbidity of long rods that fit this description is

$$\tau_{rod} = [88\pi^3 n_o(\partial n/\partial C)_\mu^2/(15N_A\lambda^3)]MC/L \quad (A.5)$$

(Gaskin et al., 1974; Berkowitz and Day, 1980).

The particle scattering factor for polydisperse, randomly oriented random coils has been described for a weight-average degree of polymerization of $\langle n\rangle$ and a distribution function of M equal to

$$(y^{z+1}/z!)M^z e^{-yM}, \quad (A.6)$$

where y is equal to $(z + 1)/\langle n\rangle$ and z is an adjustable parameter (Zimm, 1948b; Geiduschek and Holtzer, 1958). For z equal to 1, the particle scattering factor for polydisperse, randomly oriented, long random coils with a weight-average radius of gyration, $\langle R_G\rangle$, that is much greater than λ/n_o, is

$$P(\theta) = 2/(2 + x), \quad (A.7)$$

where x equals $(4\pi n_o\langle R_G\rangle\sin(\theta/2)/\lambda)^2$ (Zimm, 1948b; Doty and Steiner, 1950). (Using the z-average radius of gyration gives $P(\theta)$ equal to $3/(3 + x)$ (Geiduschek and Holtzer, 1958).) Equation A.7 results in

$$Q = (3/2)([(A^2 + 2A + 2)/A^3] \times [\ln(1 + A)] - [(2 + A)/A^2]), \quad (A.8)$$

where A equals $(4\pi n\langle R_G\rangle/\lambda)^2/2$ (Doty and Steiner, 1950). At sufficiently large $\langle R_G\rangle$, Q equals $[3/2][1/A][\ln(1 + A) - 1]$, and the turbidity, for B equal to zero, becomes

$$\tau_{coil} = (\ln[(\lambda^2 + 8\pi^2 n_o^2\langle R_G\rangle^2)/\lambda^2] - 1) \times [2\pi(\partial n/\partial C)_\mu^2/(N_A\lambda^2)]\langle M\rangle C/\langle R_G\rangle^2, \quad (A.9)$$

where $\langle M\rangle$ is the weight-average molar mass. For λ between 326 and 686 nm, Eq. A.9 works well if $\langle R_G\rangle$ is greater than or equal to 6.105×10^{-4} cm.

Long rods that are part of the coagulin gel can be thought of as having arbitrarily large values of L and M. Thus, to calculate the turbidity due to long rods in a gel, it is desirable to eliminate M and L from Eq. A.5. This can be accomplished by replacing M/L with a constant. M/L varies with the degree of lateral association, F, however. The problem can be surmounted by picking a constant, κ_{rod}, equal to M/L at F equal to 1. The turbidity of any species of long rod, i, then becomes

$$\tau_i = [88\pi^3 n_o(\partial n/\partial C)_\mu^2/(15N_A\lambda^3)C_i\kappa_{rod}F_i, \quad (A.10)$$

and the total turbidity due to all long rods (approximated as a linear sum) becomes

$$\tau_{rod} = \Sigma\tau_i = [88\pi^3 n_o(\partial n/\partial C)_\mu^2/(15N_A\lambda^3)\kappa_{rod}\Sigma C_i F_i \quad (A.11)$$

or

$$\tau_{rod} = \Sigma\tau_i = [88\pi^3 n_o(\partial n/\partial C)_\mu^2/(15N_A\lambda^3)C\kappa_{rod}\langle F\rangle, \quad (A.12)$$

where $\langle F\rangle$ is the weight-average degree of lateral association and C equals Σc_i. In Eq. A.12, τ_{rod} is proportional to $C\langle F\rangle$ at any given wavelength.

The molar mass of the coagulin monomer is 16,582 g/mol. The ratio of M to L for the model coagulin protofibril shown in Fig. 5 is

$$\kappa_{rod} = M/L = (4 \cdot 16{,}582 \text{ g/mol})\langle F\rangle/[(2 + \sqrt{2})r], \quad (A.13)$$

where $\langle F\rangle$ equals the weight-average of the number of laterally associated protofibrils. For the protofibril itself, F equals 1. The radius of the monomer, r, is 1.702×10^{-7} cm. The amount by which one protofibril laterally overlaps

another is $4r - (2 - \sqrt{2})r = (2 + \sqrt{2})r$. The protofibrils can be classified as long rods and treated by Eq. A.5 if their length is over 3.5 times the wavelength of the light scattered (Timasheff, 1981). Using Eq. A.13, it can be seen that protofibrils consisting of 783 or more coagulin monomers would fit this criterion for light with a wavelength of 326 nm. At or above that wavelength, a small oligomer with the same mass:length ratio as the protofibril, such as the 22 mer of the model described in the Discussion, is treated as a small particle.

Long random coils that are part of the coagulin gel can be thought of as having arbitrarily large values of R_G and M. Thus, to calculate the turbidity due to long random coils in a gel, it is desirable to eliminate $\langle M\rangle$ and $\langle R_G\rangle$ from Eq. A.9. Unfortunately, R_G appears twice in Eq. A.9, and it does not have the same relationship to M in both places. Nevertheless, $\langle M\rangle/\langle R_G\rangle^2$ can be replaced with a constant, and R_G in the logarithmic term can be given a value that is large enough to justify the use of the equation. Like M/L, $\langle M\rangle/\langle R_G\rangle^2$ varies with the degree of lateral association, Y, so a constant, κ_{coil}, is picked that is equal to $\langle M\rangle^{1/2}/\langle R_G\rangle$ at Y equal to 1. The turbidity of any species of long random coils, i, then becomes

$$\tau_i = (\ln[(\lambda^2 + 8\pi^2 n_o^2\langle R_G\rangle^2)/\lambda^2] - 1) \times [2\pi(\partial n/\partial C)_\mu^2/(N_A\lambda^2)])C_i\kappa_{coil}^2 Y_i, \quad (A.14)$$

and the total turbidity due to all long random coils (approximated as a linear sum) becomes

$$\tau_{coil} = \Sigma\tau_i = (\ln[(\lambda^2 + 8\pi^2 n_o^2\langle R_G\rangle^2)/\lambda^2] - 1) \times [2\pi(\partial n/\partial C)_\mu^2/(N_A\lambda^2)])\kappa_{coil}^2\Sigma C_i Y_i \quad (A.15)$$

or

$$\tau_{coil} = \Sigma\tau_i = (\ln[(\lambda^2 + 8\pi^2 n_o^2\langle R_G\rangle^2)/\lambda^2] - 1) \times [2\pi(\partial n/\partial C)_\mu^2/(N_A\lambda^2)])C\kappa_{coil}^2\langle Y\rangle, \quad (A.16)$$

where $\langle Y\rangle$ is the weight-average degree of lateral association and C equals Σc_i. In Eq. A.16, τ_{coil} is proportional to $C\langle Y\rangle$ at any given wavelength, provided that a fixed value is chosen for $\langle R_G\rangle$. For this paper, $\langle R_G\rangle$ was fixed at 6.105×10^{-4} cm in all calculations of τ_{coil}.

For the random coil,

$$\kappa_{coil} = \frac{\langle M\rangle^{1/2}}{\langle R_G\rangle} = \frac{[(4 \cdot 16{,}582\ \text{g/mol})Y]^{1/2}}{[(2 + \sqrt{2})r][2(\sqrt{2})/\pi]/\sqrt{6}}. \quad (A.17)$$

The factor $2(\sqrt{2})/\pi$ introduces an effect of flexibility on the distance between any two points of the random coil. It is a rough estimate based on electron micrographs of the gel (Holme and Solum, 1973; Moody, 1994). The factor $(2 + \sqrt{2})r$ is as defined in Eq. A.13. The length in the denominator, $[(2 + \sqrt{2})r][2(\sqrt{2})/\pi]$, is the contribution that the mass-related term in the numerator, $(4 \times 16{,}582$ g/mol$)Y$, makes to the weight-average root mean square of the distance between the ends of the coil. That length divided by $\sqrt{6}$ is the contribution that the term $(4 \times 16{,}582$ g/mol$)Y$ makes to the weight-average radius of gyration.

The turbidity due to the reflective regions is calculated as

$$\tau_\pi = \langle J\rangle\kappa_\pi C \ln(1/[1 - \langle r\rangle]), \quad (A.18)$$

where $\langle J\rangle$ is the weight-average degree of lateral association, κ_π is a constant (for the model in this paper, it is given a value of 30,000 cm^2/g), C is the mass concentration of the reflective regions, and $\langle r\rangle$ is the average reflection coefficient. In Eq. A.18, τ_π is proportional to $C\langle J\rangle$ at any given wavelength.

Any reflection coefficient, r, is equal to I_r/I_o, where I_o is the intensity of the incident light striking the reflective surface and I_r is the intensity of the reflected light (Feynman, 1965). To make τ_π proportional to $\ln(I_o/I)$, where I_o and I are given in terms of r, it was assumed that (I_o/I) equals $(I_o/[I_o - I_r])$, which, in turn, equals $(1/[1 - r])$. The term $\ln(1/[1 - \langle r\rangle])$ is considered equal to the turbidity of a single, irregular but unbroken surface or film of the protein in the solvent. The angle of the surface with respect to the direction of propagation of the incident light was assumed to vary randomly from 0 to $\pi/2$ radians with position on the surface. It was further assumed that the turbidity of the presumably discontinuous surfaces of the reflective regions should be proportional to their total surface area, and that their total surface area could be treated as proportional to their mass concentration. Thus, $\ln(1/[1 - \langle r\rangle])$ is multiplied by a mass concentration term for the reflective regions. This requires multiplication by a constant, κ_π, in units of cm^2/g for τ_π to have the proper units.

The reflection coefficient for incident light with a direction of propagation perpendicular to the reflecting surface (the angle of incidence, θ_i, is equal to zero) is

$$r_{norm} = [(n_2 - n_o)/(n_2 + n_o)]^2, \quad (A.19)$$

where n_o is the refractive index of the medium (in this case, the solvent) and n_2 is the refractive index of the material (in this case, the protein) (Feynman, 1965). The refractive index of coagulin is estimated as $n_2 = n_o + \bar{\nu}_2(\partial n/\partial C)_\mu$, where $\bar{\nu}_2$, the partial specific volume of coagulin, is estimated from centrifugation studies to be 0.738 cm^3/g (data not shown). Treating the protein as the medium and the solvent as the material gives the same results for r_{norm} as would be obtained using Eq. A.19 as written. For θ_i not equal to zero, the reflection coefficient for polarized incident light with the electric field perpendicular to the plane of incidence is

$$r_\perp = [\sin(\theta_i - \theta_t)/\sin(\theta_i + \theta_t)]^2, \quad (A.20)$$

and the reflection coefficient for polarized incident light with the electric field parallel to the plane of incidence is

$$r_\parallel = [\tan(\theta_i - \theta_t)/\tan(\theta_i + \theta_t)]^2, \quad (A.21)$$

where θ_t is the angle of the transmitted beam (Feynman, 1965). Snell's law is used to obtain θ_t in terms of θ_i (Feynman, 1965):

$$\theta_t = \arcsin[n_o \sin(\theta_i)/n_2]. \quad (A.22)$$

The average reflection coefficient for unpolarized incident light and all possible angles of incidence was estimated as

$$\langle r\rangle = \int [r_{norm} + (r_\perp + r_\parallel)/2]d\theta_i(\pi/2), \quad (A.23)$$

where the limits of integration are from 0 to $\pi/2$ radians. It is approximated that the same value of $\langle r\rangle$ would be obtained in the case of $\theta_t = \arcsin[n_2\sin(\theta_i)/n]$. A Cauchy-like relationship was then found for Eq. A.23, which gives

$$\langle r\rangle = g_1(g_2 + g_3/\lambda^2), \quad (A.24)$$

where $g_1 = 0.69092$, $g_2 = 0.14219$, and $g_3 = 1.38120 \times 10^{-11}$ cm^2.

The total turbidity of a solution of small particles, long rods, long random coils, and reflective regions was approximated as

$$\tau_{total} = \tau_{small} + \tau_{rod} + \tau_{coil} + \tau_\pi, \quad (A.25)$$

where, for i species of small particles, $\tau_{small} = [32\pi^3 n_o^2(\partial n/\partial C)_\mu^2/(3N_A\lambda^4)]\Sigma M_i C_i$. The wave length exponent for such a solution was calculated as

$$w = d\ln\tau_{total}/d\ln\lambda = (\lambda/\tau_{total})(d\tau_{total}/d\lambda). \quad (A.26)$$

For the purpose of this paper, the weight-averaged degree of lateral association of the long rods was considered to be equal to that of the long random coils and that of the reflective regions. Thus they are all denoted in the discussion as $\langle X\rangle$ ($\langle X\rangle = \langle F\rangle = \langle Y\rangle = \langle J\rangle$).

We cannot thank Alfred Holtzer and Bruno H. Zimm enough for their help in trying to make sense of our experimental results.

This research was supported in part by National Science Foundation grants BIR-9314040, DIR-9002027, and DIR-8914571. This paper is Scientific Contribution 1930 from the New Hampshire Agricultural Experiment Station.

REFERENCES

Andreu, J., and S. N. Timasheff. 1986. The measurement of cooperative protein self-assembly by turbidity and other techniques. *Methods Enzymol.* 130:47–59.

Bang, F. B. 1956. A bacterial disease of *Limulus polyphemus*. *Bull. Johns Hopkins Hosp.* 98:325–337.

Berkowitz, S. A., and L. A. Day. 1980. Turbidity measurements in an analytical ultracentrifuge. Determinations of mass per length for filamentous viruses fd, Xf, and Pf3. *Biochemistry.* 19:2696–2702.

Camerini-Otero, R. D., and L. A. Day. 1978. The wavelength dependence of the turbidity of solutions of macromolecules. *Biopolymers.* 17: 2241–2249.

Camerini-Otero, R. D., R. M. Franklin, and L. A. Day. 1974. Molecular weights, dispersion of refractive index increments, and dimensions from transmittance spectrophotometry. Bacteriophages R17, T7, and PM2, and tobacco mosaic virus. *Biochemistry.* 13:3763–3773.

Cancellieri, A., C. Frontali, and E. Gratton. 1974. Dispersion effect on turbidimetric size measurement. *Biopolymers.* 13:735–743.

Cantor, C. R., and P. R. Schimmel. 1980. Other scattering and diffraction techniques. *In* Biophysical Chemistry. Part II: Techniques for the Study of Biological Structure and Function. W. H. Freeman and Co., San Francisco. 838–846.

Casassa, E. F., and H. Eisenberg. 1964. Thermodynamic analysis of multicomponent solutions. *Adv. Protein Chem.* 19:287–395.

Castellan, G. W. 1983. Polymers. *In* Physical Chemistry. Addison-Wesley Publishing Co., Reading, MA. 929–935.

Cheng, S. M., A. Suzuki, G. Zon, and T. Y. Liu. 1986. Characterization of a complementary deoxyribonucleic acid for the coagulogen of *Limulus polyphemus*. *Biochim. Biophys. Acta.* 868:1–8.

Chou, R. R., M. H. Stromer, R. M. Robson, and T. W. Huiatt. 1990. Determination of the critical concentration required for desmin assembly. *Biochem. J.* 272:139–145.

Debye, P. 1954. Angular dissymmetry of scattering and shape of particles. *In* The Collected Papers of Peter J. W. Debye. Interscience, New York. 500–513.

De Cristofaro, R., and E. Di Cera. 1991. Phenomenological analysis of the clotting curve. *J. Protein Chem.* 10:455–468.

Donovan, M. A. 1990. Initial characterization of coagulogen polymerization and a novel trypsin inhibitor from *Limulus polyphemus*. Ph.D. dissertation. University of New Hampshire, Durham, NH.

Donovan, M. A., and T. M. Laue. 1991. A novel trypsin inhibitor from the horseshoe crab *Limulus polyphemus*. *J. Biol. Chem.* 266:2121–2125.

Doty, P., And R. F. Steiner. 1950. Light scattering and spectrophotometry of colloidal solutions. *J. Chem. Phys.* 18:1211–1220.

Feynman, R. P. 1965. Reflection from surfaces. *In* The Feynman Lectures on Physics, Vol. 2. R. P. Feynman, R. B. Leighton, and M. Sands, editors. Addison Wesley Publishing Co., Reading, MA. 33.

Gaffin, S. L. 1976. The clotting of the lysed white cells of *Limulus* induced by endotoxin. I. Preparation and characterization of clot-forming proteins. *Biorheology.* 13:237–280.

Gaskin, F., C. Cantor, M. Shelanski, and B. Berne. 1974. Turbidimetric studies of the in vitro assembly and disassembly of porcine neurotubules. *J. Mol. Biol.* 89:737–758.

Geiduschek, E. P., and A. Holtzer. 1958. Application of light scattering to biological systems: deoxyribonucleic acid and the muscle proteins. *Adv. Biol. Med. Phys.* 6:431–551.

Hantgan, R. R., and J. Hermans. 1979. Assembly of fibrin: a light scattering study. *J. Biol. Chem.* 254:11272–11281.

Hantgan, R., J. McDonagh, and J. Hermans. 1983. Fibrin assembly. *Ann. N.Y. Acad. Sci.* 408:344–366.

Holme, R., and N. O. Solum. 1973. Electron microscopy of the gel protein formed by clotting of *Limulus polyphemus* hemocyte extracts. *J. Ultrastruct. Res.* 44:329–338.

Johnson, K. A., and G. G. Borisy. 1979. Thermodynamic analysis of microtubule self-assembly in vitro. *J. Mol. Biol.* 133:199–216.

Laemmli, U. K. 1970. Cleavage of structural proteins during the assembly of the head of bacteriophage T4. *Nature.* 227:680–685.

Liu, T., R. C. Seid, J. Tai, S. Liang, T. P. Sakmar, and J. B. Robbins. 1979. Studies on *Limulus* lysate coagulating system. *In* Biomedical Applications of the Horseshoe Crab (*Limulidae*). E. Cohen, editor. Alan R. Liss, New York. 147–158.

Miyata, T., M. Hiranaga, M. Umezu, and S. Iwanaga. 1983. The complete amino acid sequence of coagulogen isolated from *Limulus polyphemus* amebocytes. *Ann. N.Y. Acad. Sci.* 408:651–654.

Miyata, T., M. Hiranaga, M. Umezu, and I. Sadaaki. 1984. Amino acid sequence of the coagulogen from *Limulus polyphemus* hemocytes. *J. Biol. Chem.* 259:8924–8933.

Moody, T. P. 1994. Physical studies of *Limulus* coagulogen, the coagulin gel and coagulin gel formation. Ph.D. dissertation. University of New Hampshire, Durham, NH.

Nakamura, S., S. Iwanaga, T. Harada, and M. Niwa. 1976. A clottable protein (coagulogen) from amoebocyte lysate of Japanese horseshoe crab (*Tachypleus tridentatus*). *J. Biochem.* 80:1011–1021.

Oosawa, F., and S. Asakura. 1975. Energetics. *In* Thermodynamics of the Polymerization of Protein. Academic Press, London. 56–69.

Rawn, J. D. 1983. Enzyme kinetics. *In* Biochemistry. Harper and Row, New York. 225–267.

Shishikura, F., S. Nakamura, K. Takahashi, and K. Sekiguchi. 1982. Horseshoe crab phylogeny based on amino acid sequences of the fibrinopeptide-like peptide C. *J. Exp. Zool.* 223:89–91.

Shishikura, F., S. Nakamura, K. Takahashi, and K. Sekiguchi. 1983. Coagulogens from four living species of horseshoe crab (*Limulidae*): comparison of their biochemical and immunochemical properties. *J. Biochem.* 94:1279–1287.

Solum, N. O. 1970. Some characteristics of the clottable protein of *Limulus polyphemus* blood cells. *Thromb. Diath. Haemorrh.* 23:170–181.

Solum, N. O. 1973. The coagulogen of *Limulus polyphemus* hemocytes. A comparison of the clotted and non-clotted forms of the molecule. *Thromb. Res.* 2:55–70.

Tai, J. T., R. C. Seid, Jr., R. D. Huhn, and T. Y. Liu. 1977. Studies on *Limulus* amoebocyte lysate. II. Purification of the coagulogen and the mechanism of clotting. *J. Biol. Chem.* 252:4773–4776.

Takagi, T., Y. Hokama, T. Morita, S. Iwanaga, S. Nakamura, and M. Niwa. 1979. Amino acid sequence studies on horseshoe crab (*Tachypleus tridentatus*) coagulogen and the mechanism of gel formation. *In* Biomedical Applications of the Horseshoe Crab (*Limulidae*). E. Cohen, editor. Alan R. Liss, New York. 169–184.

Tanford, C. 1961. Light scattering. *In* Physical Chemistry of Macromolecules. John Wiley and Sons, New York. 275–316.

Timasheff, S. N. 1981. The self-assembly of long rodlike structures. *In* Protein-Protein Interactions. C. Frieden and L. W. Nichol, editors. John Wiley and Sons, New York. 315–336.

van de Hulst, H. C. 1957. Introduction. *In* Light Scattering by Small Particles. John Wiley and Sons, New York. 3–10.

van Holde, K. E. 1985. Scattering. *In* Physical Biochemistry. Prentice-Hall, Englewood Cliffs, NJ. 203–234.

Weisel, J. W., C. Nagaswami, and L. Makowski. 1987. Twisting of fibrin fibers limits their radial growth. *Proc. Natl. Acad. Sci. USA.* 84: 8991–8995.

Zimm, B. H. 1948a. The scattering of light and the radial distribution function of high polymer solutions. *J. Chem. Phys.* 16:1093–1098.

Zimm, B. H. 1948b. Apparatus and methods for measurement and interpretation of the angular variation of light scattering: preliminary results on polystyrene solutions. *J. Chem. Phys.* 16:1099–1116.